BOLETIN DE LA SOCIEDAD ESPAÑOLA DE
Cerámica y Vidrio
www.elsevier.es/bsecv

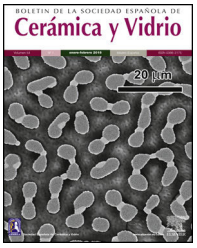

Original

Manufacturing porcelain components by CIM: Viability of processing different ceramic powders

*Cristina Berges, Alberto Gallego, Juan Alfonso Naranjo, Gemma Herranz**

Universidad de Castilla – La Mancha, INEI-E.T.S.I. INDUSTRIALES, Av. Camilo José Cela s/n, 13071 Ciudad Real, Spain

ARTICLE INFO

Article history:
Received 11 December 2019
Accepted 7 April 2020
Available online 20 April 2020

Keywords:
Ceramic Injection Moulding
CIM
Porcelains
Microstructure
Sintering
Mechanical characterization

ABSTRACT

Ceramic Injection Moulding (CIM) is an advanced powder processing technology launched three decades ago which has become a growing attractive alternative for new technical applications, such as thermal management and wireless charging. Porcelain-type ceramics can allow the introduction of new feedstocks into the CIM market at a competitive cost, in comparison with the conventional alumina and zirconia feedstocks. During the CIM manufacturing process, several factors related to the starting powder characteristics have an influence on the quality and properties of the final components, such as the mixing behaviour and the feedstock flow properties, as well as injection, debinding and sintering parameters. In this work, the viability of three porcelain-based powders to successfully achieve injectable mixtures for CIM is described. The mixing behaviour and the feedstocks flow behaviour as a function of its solids loading is evaluated. In this way, the ideal attributes for a CIM porcelain powder are discussed, studying the first process stages through to the production of a sintered component by injection moulding. Finally, density, hardness, bending strength and microstructural properties of the selected porcelain are investigated and a cost-efficient ceramic feedstock is suggested for aesthetic and electrical applications.

Fabricación de componentes de porcelana mediante CIM: viabilidad de procesado de diferentes polvos cerámicos

Palabras clave:
Moldeo por inyección de cerámicas
CIM
Porcelanas
Microestructura
Sinterización
Caracterización mecánica

RESUMEN

El moldeo por inyección de cerámica (en inglés, Ceramic Injection Moulding [CIM]) es una tecnología avanzada de conformado de polvos establecida hace tres décadas que recientemente se ha convertido en una atractiva alternativa para nuevas aplicaciones avanzadas, como la gestión térmica y la recarga inalámbrica de dispositivos. Las cerámicas de tipo porcelana permiten la introducción de nuevos *feedstocks* en el mercado CIM a precios más bajos en comparación con los tradicionales de alúmina y zircona. Existen varios factores que influyen en la calidad y las propiedades de los componentes finales en el procesado CIM y que están relacionados con las características del polvo de partida, como son el

* *Corresponding author.*
E-mail address: gemma.herranz@uclm.es (G. Herranz).
https://doi.org/10.1016/j.bsecv.2020.04.001

comportamiento durante el mezclado y la fluidez del *feedstock*, así como los parámetros de inyección, eliminación y sinterización. En este trabajo se describe la viabilidad de tres porcelanas para obtener mezclas inyectables que puedan procesarse con éxito mediante CIM. Se muestra la estabilización del par de torsión durante el proceso de mezclado, así como la fluidez de los diferentes *feedstocks* en función de la carga cerámica. Asimismo, se discuten las cualidades que idealmente se buscan en un polvo para ser procesados mediante CIM. Finalmente, se muestran los resultados obtenidos de densidad, propiedades microestructurales y propiedades mecánicas (dureza y resistencia a la flexión) de la porcelana seleccionada, y se demuestra que la mezcla inyectable diseñada a precio competitivo puede utilizarse para aplicaciones estéticas y eléctricas en futuros trabajos.

Introduction

Powder Injection Moulding (PIM) technology (or Ceramic Injection Moulding, CIM, for ceramic materials) in industry has experienced a remarkable increment in the last decades, allowing shaping complex geometries for lower production costs and reducing the necessity of post-treatments [1]. CIM process comprises multiple stages, starting with mixing the selected powder and binder system, usually based on thermoplastic polymers, to produce the initial injectable mixtures, also called feedstocks. Then, the injection moulding machine is fed with the optimized feedstock pellets, which are heated and pressured, so the mould can be filled in an adequate way. After cooling, the component with the desired geometry is ejected. Debinding of the resulting green parts is performed by a solvent, by a thermal or catalytic process (depending on the used binder) and a residual binder amount is left for holding powder particles. Brown parts are finally sintered upon temperature leading to high-densified components with its corresponding dimensional shrinkage. In this context, feedstock formulation with optimal solids loading is crucial, since enough binder is required to provide fluidity during moulding, but too much binder may cause shape lost during debinding [2,3].

In a world where ceramic materials have emerged as unique candidates for advanced engineering applications such as thermal management and wireless charging, biomedicine and jewellery applications, the development of CIM process has been limited by the lack of commercially available injectable mixtures that suit the requirements of the ceramic industry. Typically, the most common feedstocks that manufacturing companies can access are based on high-cost alumina and zirconia powders, especially designed to high-tech and luxury sectors. Porcelains, on the contrary, present remarkable mechanical, electrical and aesthetic properties while considerably reducing the starting material price and, therefore, the final feedstock cost, opening a new set of applications. These materials are available in abundance and require sintering temperatures that are significantly lower than those needed for metal oxide-based materials [4,5]. However, few studies concerning manufacturing porcelain components by CIM can be found in peer reviewed literature [6,7] and there are no commercially available porcelain feedstocks for CIM manufacturing. Other adapted processing techniques, such as aqueous injection moulding or wet pressing, have allowed some authors to report well-designed and homogeneous porcelain products [8,9].

The final component quality can be influenced by numerous aspects during the CIM process. The mixing behaviour, feedstock solids loading, feedstock flow properties, injection moulding parameters, debinding rate, sintering response or dimensional control are some of them. Most of these factors are mainly dominated by powder properties, such as particle size, particle shape and particle size distribution. Indeed, for ideal CIM processing, a balance between several factors needs to be reached, which are often contradictory. For example, spherical particles favours not only moulding, higher solids loadings and faster sintering but also more agglomeration and sintering shrinkage, while irregular particles increase the component strength after binder removal and raise the mixture viscosity [3]. On the other hand, the feedstock composition in terms of solids loading directly affects the viscosity of the mixture and, therefore, the injection pressure required for the process. From an industrial point of view, high-pressure injection machines are extended due to the high production capabilities, which allow increasing the ceramic content of the injectable mixture. Therefore, when designing a novel feedstock for CIM, the equipment involved in further steps of the process need to be also considered. For example, the use of a low-pressure injection machine could have different requirements in terms of viscosity due to the lower pressure achieved.

In this context, the present work aims to develop new ceramic-binder injectable mixtures containing porcelain powders to be processed by CIM. Several porcelain powders with different composition, morphology and particle size distribution have been tested by mixing with the same binder system and varying the ceramic solids loading. Differences on mixing behaviour, flow rate and injection response were analyzed and porcelain feedstock showing the best properties to continue with the following steps of CIM process were selected. Two commercially available porcelain powders and one composition especially adjusted and conditioned for CIM technology have been employed in the study. The influence of the different particle sizes and distributions on the CIM parameters was discussed. Moreover, the scale up of the selected composition was performed adjusting the feedstock's ceramic content, as well as the injection conditions, in order to transfer the material to an industrial production process. Finally, sintered parts

Table 1 – Chemical composition (wt.%), particle size (D_{10}, D_{50} and D_{90}) and density determined for each studied powder.

	Al_2O_3	SiO_2	Fe_2O_3	TiO_2	K_2O	Otros	D_{10} (μm)	D_{50} (μm)	D_{90} (μm)	ρ (g/cm³)
P1	40–45	35–55	≤2.1	≤2.1	–	≤1	0.74	2.0	4.4	2.61
P2	26	71	0.5	0.6	1	0.8	0.70	8.7	49	2.54
P3	69–70	26–27	0.2		2.9	1	1.4	7.4	36	3.25

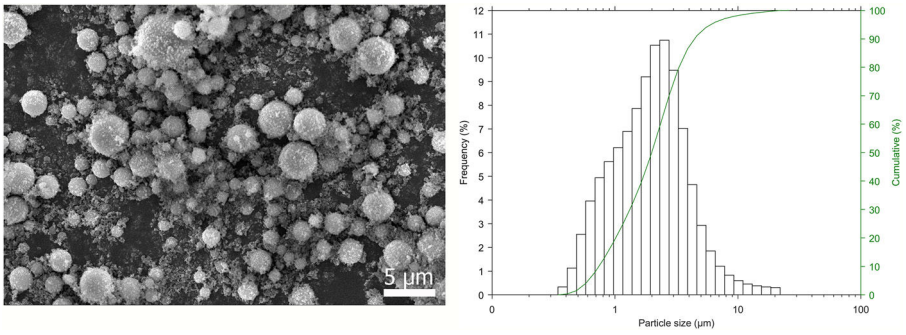

Fig. 1 – SEM micrograph (left) and particle size distribution (right) of porcelain P1.

were characterized in terms of apparent density, hardness, bending strength and microstructural analysis.

Experimental part

Characterization of the raw materials

Three different porcelains, named as P1, P2 and P3, and a thermoplastic-based binder composed of High Density Polyethylene (HDPE), paraffin wax and stearic acid, were utilized as raw materials in the present study. P1 and P2 were commercially available porcelain powders and P3 was fabricated and adapted for CIM processing by Vicar S. A. Regarding the binder system, HDPE (0.9390 g/cm³) was supplied from Chemieuro S. L. and paraffin wax (0.9086 g/cm³) and stearic acid (1.0023 g/cm³) from Panreac Applichem.

The chemical composition of the three porcelain-type powders was provided by the supplier (see Table 1). Additionally, granulometry and density were evaluated, and the summarized data are also displayed in Table 1. Granulometry was analyzed with a Micromeritics Sedigraph 5100 measuring in a range from 300 to 0.10 μm of equivalent spherical diameter. A Helium Pycnometer (Micrometrics Accupyc II 1340) was used to analyze density values, performing several tests of each material to ensure reproducibility. On the other hand, the morphology characterization of the different porcelains was carried out by Scanning Electron Microscopy (SEM) using the equipment JEOL model JSM-6610LV. Samples were coated with a gold film by sputtering using a Cressington Sputter Coater 108 Auto.

The results regarding microstructure and granulometric characterization are shown in Figs. 1–3. Porcelain P1 displays a spherical morphology, while an irregular partially angular shape and an irregular morphology are observed for P2 and P3, respectively. The particle size estimated by SEM micrographs in each case are in good accordance with the results obtained after the granulometric measurements listed in Table 1. As noted in the table, the average particle size (D_{90}) of P1 is the smallest value of those studied, 4.4 μm, and the granulometric analysis shows a narrow monomodal near-gaussian distribution of the particle size (see Fig. 1 right). In the case of P2, the particle size does not follow a gaussian distribution (Fig. 2 right) showing the highest value of D_{90} (49 μm). Finally, P3 also presents a near-gaussian distribution, as is confirmed in the granulometric studies (Fig. 3 right) and a broader particle size distribution than P1, having $D_{90} \leq 36$ μm.

Experimental procedure

Porcelain feedstocks were prepared by mixing the different porcelain powders with a multicomponent binder system containing HDPE, paraffin wax (PW) and stearic acid (SA), formulated in the following ratio with respect to the vol. % of binder content: 30, 65 and 5 vol.%, respectively (see Table 2). Several ceramic solid loadings in the range of 45–55 vol.% were tested in order to choose the best option.

Feedstock compounding was performed in a double rotor Thermo Scientific Haake PolyLab OS-System mixer, using the following experimental conditions: temperature of 160 °C (according to the thermal properties of the binder system), rotational speed of 30–70 rpm and durations between 80 and 300 min, depending on the feedstock homogenization. The mixing process was carried out by adding several fractions of the components into the mixer during the first 30 min and then, the mixture was left to homogenize. The torque evolution with time was monitored and the feedstock was obtained after milling and sieving in a Restch SM 100 mill.

Feedstock flow behaviour was studied by using a Melting Flow Index (MFI) equipment, Dynisco LMI 500 Series, determining flow rate values according to standard UNE-EN ISO 1133-1. The procedure consisted of extruding the melt material through a cylinder with specific length and diameter, setting temperature and load in each test. Injection stage was carried out in a low-pressure injection machine in the first stage: AB Machinery model AB-400 M varying the

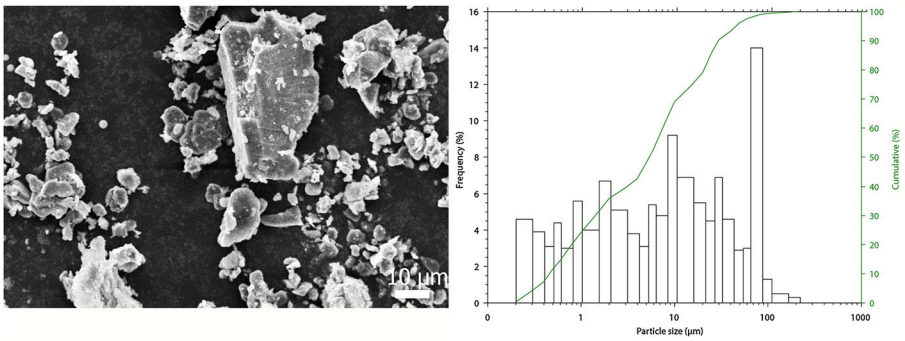

Fig. 2 – SEM micrograph (left) and particle size distribution (right) of porcelain P2.

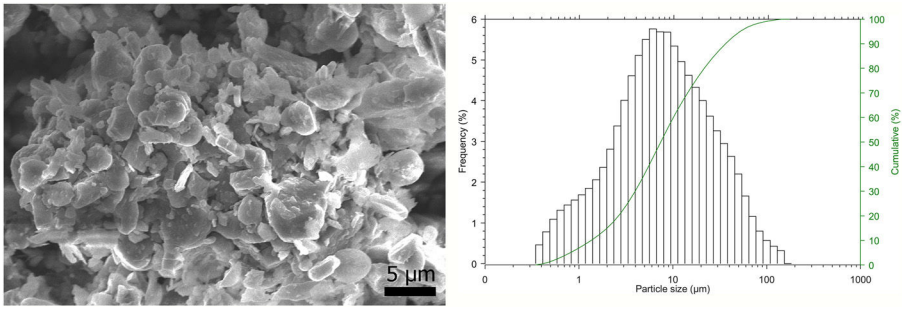

Fig. 3 – SEM micrograph (left) and particle size distribution (right) of porcelain P3.

Table 2 – Feedstock formulations.

Porcelain	Solids loading (vol.%)	HDPE (vol.%)	Paraffin wax (vol.%)	Stearic acid (vol.%)	Binder ratio (vol.%) (HDPE:PW:SA)
P1	45	13.5	29.25	2.25	30:65:5
P2	45	13.5	29.25	2.25	
	48	14.4	31.2	2.4	
	50	15	32.5	2.5	
P3	45	13.5	29.25	2.25	
	50	15	32.5	2.5	
	55	16.5	35.75	2.75	
	57	17.1	37.05	2.85	

experimental conditions in the range of 150–190 °C and 115–235 bar; and in a high-pressure injection machine in the next stage: Arburg 270 s machine varying the experimental conditions in the range of 150–170 °C and 500–850 bar. The injected green parts were cuboid shaped with the following dimensions: 6.7 mm (l) × 12.2 mm (w) × 4.9 mm (h). In addition, a rheological study was carried out in a Dynisco LCR 7000 series capillary rheometer varying the temperature from 150 °C to 175 °C, at shear rates selected between 10 and 10000 s^{-1}. A die having a length/diameter ratio $L/D = 30$ and a 0–1400 bar pressure sensor were used.

Thermal debinding cycles were carried out for binder elimination in a Hobersal furnace (12PR450/SCH PAD P) between 25 °C and 440 °C under flowing air. The brown parts obtained were subsequently sintered in a tubular furnace Hobersal furnace (ST 186030) at a temperature ranging between 1290 °C and 1430 °C, which was maintained for 1 h under flowing air and then cooled down in the furnace.

The mechanical characterization was evaluated in terms of microhardness and three-point bending strength tests. The microhardness was evaluated in the sintered parts using a Vickers diamond pyramid (Digital Future-Tech series FM-7), applying a load of 9.8 N during 15 s. Three-points bending strength has been carried out in a SHIMADZU equipment (Autograph AG-X 50 kN) at a speed of 1 mm/min.

Results and discussion

Feedstock production

The first feedstock of porcelain P1 was prepared at 160 °C containing 45 vol.% of ceramic solids loading. Results concerning torque evolution over time are shown in Fig. 4 (left). It is readily apparent that torque reaches a steady state after almost 100 min of homogenization. However, the obtained feedstock did not result in a homogeneous mixture, as powder segregation was observed in the mixer (Fig. 4 (right)). During that

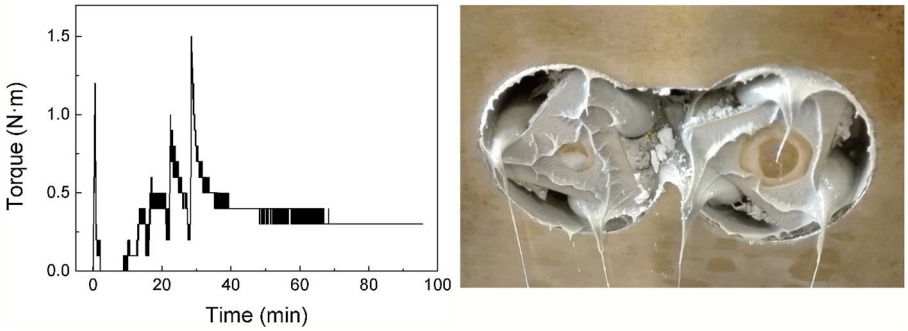

Fig. 4 – Torque change over change in mixing duration of porcelain P1 containing 45 vol.% of solids loading (left) and the resulting feedstock obtained in the mixer (right).

time, clusters of particles were not completely broken down under shear action and the binder could not surround the powder efficiently, even with the addition of a surface-active agent such as stearic acid to the binder system. Therefore, similar mixtures extending mixing times up to 300 min and increasing rotational speed up to 70 rpm were attempted, with the objective of decreasing cluster size and dispersing the binder between powder particles using only shear action, but no improved results were obtained.

These difficulties can be associated to the formation of ceramic powder agglomerates due to the effect of the small D_{10} value, together with the narrow particle size distribution. Despite its spherical morphology and small particle size with $D_{90} < 10\,\mu m$ (see Fig. 1), both features usually recommended for injection moulding and sintering steps in CIM process, the narrow monomodal particle size distribution could be harmful for packing density and flow characteristics [3,6,10,11]. This fact is currently under investigation and a surface treatment with dispersants or milling the ceramic powder are being considered in order to avoid agglomeration and ensure a homogenized mixture [3,12–14]. Another approach would be to test different binder compositions that would better suit this material, as it seems clear that the amount of stearic acid incorporated as compatibilizer was not enough. On the other hand, the small and spherical particle size observed in P1, related to a high specific area of the particles, might also imply the need of a higher amount of binder to surround the powder in an efficient way, which means a reduction of the ceramic solid loading. Since high ceramic contents are desirable for achieving high density CIM components after sintering, values of solid loading lower than 45 vol.% are not recommended. The other possibilities mentioned above, are out of the scope of the present study. For this reason, this material was discarded in the present work.

Similarly, feedstocks of porcelains P2 and P3 were also fabricated. Ceramic solids loading was varied in the range of 45–50 vol.% for P2 (P2-45 vol.%, P2-48 vol.% and P2-50 vol.%) and in the range of 45–57 vol.% for P3 (P3-45 vol.%, P3-50 vol.%, P3-55 vol.% and P3-57 vol.%). In all cases, mixing conditions were carried out at 160 °C and 30 rpm. In these cases, homogeneous mixtures were obtained under shear action, as the porcelain powder was completely incorporated into the binder system (see Fig. 5).

Table 3 – Density values obtained for feedstock P3-55 vol.% measured in the Helium Pycnometer.

Feedstock	Density (g/cm³) ± std. dev. (g/cm³)
P3-55 vol.%	2.2205 ± 0.0010
	2.2157 ± 0.0011
	2.2186 ± 0.0009
	2.2098 ± 0.0014
	2.2112 ± 0.0011

Density measurements of several feedstock fractions with the Helium Pycnometer allowed to get further confirmation of the achieved feedstock homogenization. It is accepted that larger variation between density values than ± 0.020 g/cm³ results in a lack of homogeneity [15–18]. In all the current cases, density variation was lower than ± 0.020 g/cm³. As an example, the results obtained in the case of mixture P3-55 vol.% are shown in Table 3, where a density variation lower than ± 0.0011 g/cm³ in average was found after five tests of different material fractions.

Optimal solids loading selection

It is well known that a balanced powder:binder ratio is a decisive factor for CIM process success. Each powder requires a specific binder concentration range, depending on its particle size distribution and particle shape. When the ceramic powder is mixed with the binder, the “critical solids loading” situation corresponds to powder particles in point contact while the remaining free space is filled with binder. However, moulding is preferably carried out at a slightly higher binder amount, corresponding to the so called “optimal solids loading” [3].

With the objective of selecting optimal solids loading of the previously designed powder-binder mixtures of porcelains P2 and P3, several aspects have been jointly considered. The aim is to reach homogeneous mixing behaviour, flow rate in an adequate range and keep the powder concentration (vol.%) as high as possible, in order to provide better shrinkage control during debinding and sintering.

Torque evolution over time was tracked in P2 and P3 porcelain feedstocks during the mixing process, having powder loadings in the range of 45–50 vol.% and 45–57 vol.%, respectively (Fig. 6). Torque fluctuations upon additions usually finish when powder and binder are uniformly distributed.

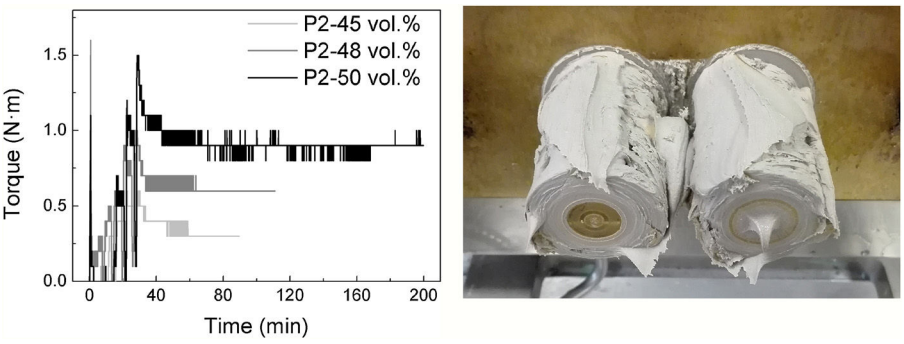

Fig. 5 – Appearance of feedstocks obtained after the mixing process for porcelain P2-48 vol.% (left) and porcelain P3-55 vol.% (right).

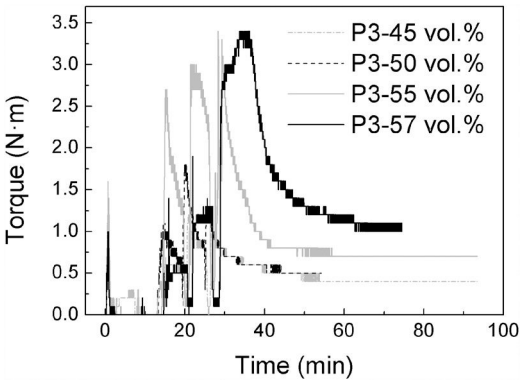

Fig. 6 – Torque evolution with time during mixing process of porcelain P2 with 45, 48 and 50 vol.% solids loading (left) and porcelain P3 with 45, 50, 55 and 57 vol.% solids loading (right).

Higher torque values after reaching the steady state are found with the increment of powder concentration. This is related associated with a lower flow rate of higher loaded mixtures, as discussed below [16,19,20]. On the other hand, and additionally to the density measurements detailed previously, feedstock homogeneity is evaluated by considering the steady-state torque values after monitoring the torque. It is well-known that a homogeneous mixture is characterized by a constant torque [3]. In both families of porcelain feedstocks, although longer times are required for homogenization of the highest solid loading constant torque values after homogenization time are reached with both materials. In the case of P2 steady torque values in the range of 0.3 N m (for mixtures with 45%vol. of powder loading) and 0.9 N m (50%vol.) are achieved whereas in the P3 powder the torque value is between 0.4 (45%vol.) and 1 N m (57% vol.) after 80 min of mixing process.

Once the porcelain feedstocks are produced and with the aim to study a suitable flowability, the flow rate behaviour was investigated using the MFI equipment and calculating two flow parameters: the Melt Volume-Flow Rate, MVR ($cm^3/10'$) and the Melt Mass-Flow Rate values, MFR (g/10′). This study can provide valuable information to anticipate the feedstock flow behaviour and the most suitable temperature during the injection step. Accordingly, three temperatures were chosen, varying from 150 to 170 °C in agreement to the selected thermoplastic binder, and load was set at 2 and 5 kg, performing six tests of each material. In the case of P3-57 vol.%, an extra experiment with 7 kg load was also performed at 160 °C, since it presented high viscosity and, therefore, more difficulties to flow under lower loads.

All these results are gathered in Table 4, where good agreement with the conclusions previously obtained from the torque study can be noticed. MFI values decreased as the feedstock powder concentration, and therefore the torque, increased at a constant load, resulting in a higher viscosity. Accordingly, MFI values are found to increase with an applied load increment, at a constant temperature, which indicates the pseudoplastic character of the powder-binder mixtures.

However, the complexity of the injection moulding process, especially in the case of high powder content systems, introduces difficulties to establish a universal relationship between fluidity measurements at lab scale and feedstock mouldability [21,22]. Some authors have predicted the best choice depending on each specific powder and binder system [23–25]. Based on our previous experience [26–28], the selection criteria of the most suitable feedstock to continue with the next stages of the process takes into account the combination of torque evolution, flow properties and volume fraction maximization. Yet, an approximate range of MVR values regarding the results obtained with P2 and P3 mixtures can be estimated as the recommended ones in our study, being 15–35 $cm^3/10'$ for 2 kg load when a low-pressure injection machine is employed. In this way, feedstocks P2-48 vol.% and P3-55 vol.% (highlighted in Table 4) are selected as the optimal mixtures for each type of porcelain studied according to MFI and torque studies. Both has similar torque values (0.7 and 0.6 N m respectively) although it is relevant to remark that the mixture of P2 has 48% vol. of powder loading and the P3 mixture achieved 55% vol. Higher solids loadings in both cases (P2-50 vol.% and P3-57 vol.%) imply a significant reduction of the flow rate (together with a torque increment) even increasing temperature up to 170 °C, which could have a negative impact on the subsequent injection moulding process.

Further comparison between porcelain feedstocks P2 and P3 when a 2 kg load is applied at 160 °C is represented in Fig. 7. For this purpose, only MVR values were considered against solids loading formulated (vol.%). In this graph, the recommended MVR values range for low-pressure injection process

Table 4 – MVR and MFR values corresponding to the different solids-loaded feedstock obtained from porcelains P2 and P3, according to the different load and temperature conditions studied.

Feedstock	Load (kg)	Experimental conditions	MVR (cm^3/10′)	MFR (g/10′)
P2-45 vol.%	2	150 °C	28.4	61.2
	5		318.6	686.9
	2	160 °C	67.9	146.4
	5		254.4	548.5
	2	170 °C	101.1	218.0
	5		542.6	1168.6
P2-48 vol.%	2	150 °C	31.4	54.1
	5		185.4	319.6
	2	160 °C	33.7	58.1
	5		187.1	322.5
	2	170 °C	54.1	89.8
	5		287.4	495.4
P2-50 vol.%	2	150 °C	–	–
	5		30.9	66.6
	2	160 °C	–	–
	5		34.2	73.7
	2	170 °C	–	–
	5		136.4	294.1
P3-45 vol.%	2	150 °C	52.6	105.3
	5		246.5	493.5
	2	160 °C	200.7	400.4
	5		287.3	575.1
	2	170 °C	97.9	196.0
	5		413.3	827.6
P3-50 vol.%	2	150 °C	26.5	55.7
	5		155.1	326.0
	2	160 °C	43.3	91.0
	5		230.2	483.8
	2	170 °C	61.7	129.7
	5		322.3	677.4
P3-55 vol.%	2	150 °C	12.2	25.3
	5		79.3	176.1
	2	160 °C	19.1	40.2
	5		95.6	212.3
	2	170 °C	30.3	67.3
	5		101.4	225.2
P3-57 vol.%	2	150 °C	–	–
	5		–	–
	2	160 °C	–	–
	5		14.3	30.4
	7		40.1	85.2
	2	170 °C	–	–
	5		20.8	45.3

is highlighted. The inset part confirms the mixtures pseudoplasticity in all cases, showing a deviation from the linear MVR increment when the applied load is increased up to 7 kg, which is a desirable feature of feedstocks for PIM technology processing [3]. Moreover, it can be observed that the binder system is able to incorporate a higher powder concentration of P3 porcelain in relation to P2, since MVR values measured with P3-50 vol.% exceeded the MVR values of P2-48 vol.%, as previously described. This can be associated to the more angular shape of P2 powder when compared to P3, resulting in lower packing density and lower critical solids loading [3,10]. When it comes to selecting the most interesting powder to be

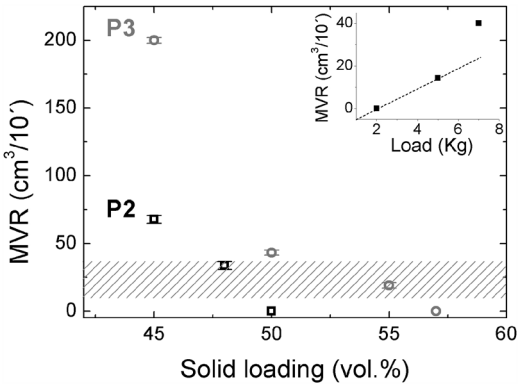

Fig. 7 – MVR values as a function of feedstocks solids loading for porcelains P2 and P3 when 2 kg load is applied at 160 °C. Inset graphic shows MVR values as a function of the applied load (2, 5 and 7 kg) obtained with feedstock P3-57 vol.% measured at 160 °C. The shadowed region at each load applied indicates an estimation range of appropriate MVR values for the low-pressure moulding injection step.

processed by CIM, all these facts previously mentioned may be detrimental in the case of P2.

Once these two P2 and P3 porcelain feedstocks, containing different powders and showing the best mixing and flow behaviour are selected, another important factor to analyze is the reproducibility of the torque evolution during the mixing process for feedstock fabrication. An appropriate powder for PIM will lead to homogeneous and reproducible feedstocks, with similar steady-state torque after a determined mixing time [29]. Fig. 8 plots torque evolution with time for feedstocks prepared up to four times with each porcelain material. The mixing behaviour of feedstock P2 is not reproducible in comparison with P3 and, consequently will present inhomogeneities, showing a higher steady torque variation in the four mixtures tested (± 0.3 N m) than that obtained in the case of P3 (± 0.1 N m). Since particle size, shape and size distribution are known to affect the mixing behaviour of the feedstocks [29], the angular shape, the bigger D_{90} value and the non-gaussian distribution could explain this result.

Low-pressure injection moulding stage

Green parts with cuboid geometry of both porcelain types were manufactured by injection moulding of the selected optimal feedstocks, at adequate temperature and pressure conditions. In the case of P2-48 vol.%, the injection process optimization implied the variation of the experimental conditions in the range of 150–190 °C of temperature and 115–235 bars of pressure. Unfortunately, superficial defects observed by visual inspection and the presence of internal pores could not be avoided, as is illustrated in Fig. 9. On the contrary, green parts of P3-55 vol.% were successfully manufactured, free of external defects and/or internal pores. The optimized injection conditions were set at 160 °C of temperature and 140 bars of pressure. The reason for such differences can be associated again to the inhomogeneities found in P2 feedstock after

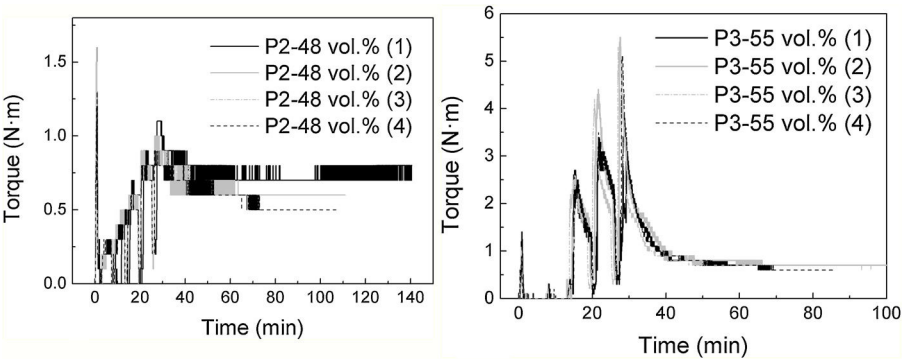

Fig. 8 – Study of reproducibility and homogeneity after several mixing processes at the same conditions of the selected optimal feedstocks P2-48 vol.% (left) and P3-55 vol.% (right).

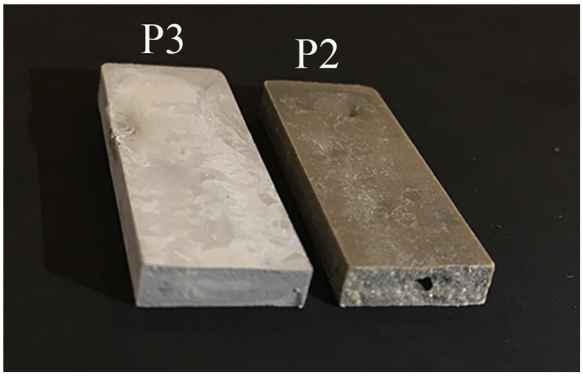

Fig. 9 – Green parts after the low-pressure injection process of P3 feedstock (left) and P2 feedstock (right).

mixing when compared to P3, due to the more angular powder shape and non-gaussian particle size distribution, as already commented [30,31]. Moreover, the lower porcelain content (48 vol.%) and higher flow rate confirmed by the MFI studies may also cause defects in moulding. Further steps of the CIM process (debinding and sintering) were then carried out only with feedstock of P3 porcelain, discarding the P2 feedstock for this work.

Reformulation of the P3 feedstock

Positive results were achieved after the low-pressure injection of P3 parts, once they were properly debound and sintered. However, the study of the novel designed P3 porcelain feedstock for high-pressure injection moulding process is required to ensure the industrial scalability since the high-pressure injection machine is more robust and able to achieve more accurate control of the injection parameters, similar to the automatization found at the industrial process. Besides, the high-pressure injection process enables the correct injection of feedstocks with higher viscosity than those available for low-pressure injection. This may favour the sintering step since a higher ceramic content can be used in the feedstock. For this reason, a slight reformulation of the feedstock is carried out. Powder loadings from 45 to 65 vol.% were prepared and both the rheological and mixing behaviour were then evaluated.

First, the viscosity dependence on shear rate, measured in a capillary rheometer, is shown in Fig. 10 (left) for all the new P3 feedstocks. As observed with the flow behaviour studied in terms of MVR values, viscosity increases with the solid loading increment. More significantly, viscosity shows a pseudoplastic behaviour (values decrease upon the shear rate increment), as determined during the MFI experiments, which confirms that the mixtures are injectable and processable by CIM. On the other hand, Fig. 10 (right) plots the steady state torque and the viscosity of each feedstock at 160 °C temperature and 1000 s^{-1} shear rate as a function of the ceramic loading. A near-linear increment of these values is observed when increasing powder loading in the mixtures up to 60 vol.%. However, a change in this trend is detected at higher powder loadings, meaning that the critical solid loading has been overcome at solid loadings higher than 60 vol.%. To ensure an adequate flow behaviour during the injection process, a reduction between 2 and 5 vol.% in the solid loading is recommended in PIM processing to allow for the normal fluctuations in particle size distribution, particle shape and mixture homogeneity in the different powder batches [3]. For this reason and applying this criterion, 57 vol.% was chosen in this work as the optimal solid loading, below the critical solid loading estimated through the rheological measurements.

High-pressure injection and debinding steps

The high-pressure injection process was then performed with the reformulated feedstock of P3 porcelain and defect-free green parts were successfully obtained, as shown in Fig. 12. The optimal injection conditions selected were 160 °C and 700 bars. Green parts were subsequently debound by the following heating cycle under flowing air: heating rate at 0.5 °C/min to 120 °C (hold 1 h), heating at 0.5 °C/min to 380 °C (hold 2 h) and again heating at 1 °C/min to 440 °C (hold 1 h) followed by furnace cooling. With this sequence, high quality brown parts were obtained containing a residual amount of binder to keep the shape.

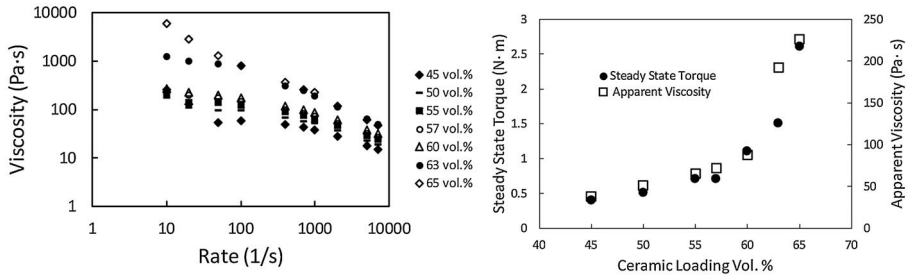

Fig. 10 – (left) Viscosity versus shear rate of the different P3 porcelain feedstocks (45–65 vol.% solid loadings) at 160 °C. (right) Comparison between torque and viscosity values obtained at 160 °C and 1000 s^{-1} for each feedstock in the solid loadings range designed (45–65 vol.%).

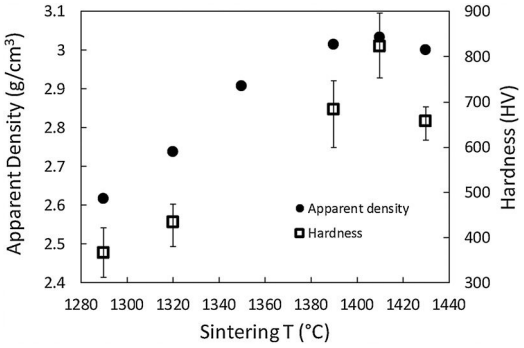

Fig. 11 – Apparent density and Vickers hardness of sintered parts at different temperatures evaluated for the optimization of the sintering stage.

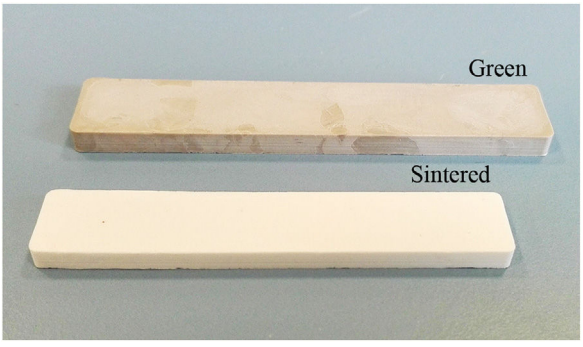

Fig. 12 – Green part (top) and sintered part at 1410 °C (bottom) of the optimal P3 porcelain feedstock processed by CIM.

Sintering, mechanical properties and microstructure characterization

Once the brown parts were produced, the sintering process was performed at different temperatures in the range of 1290–1430 °C, holding this temperature for 1 h in all cases followed by cooling in the furnace. In order to select the optimal sintering temperature, apparent density and hardness were evaluated. The densification curve for the P3 porcelain feedstock in the selected temperature range is shown in Fig. 11. The apparent density and hardness values increase up to 1410 °C after which both parameters drop, indicating that densification cannot be further improved. Thus, 1410 °C is selected as the optimal temperature for the sintering process, achieving the highest apparent density and hardness values with this porcelain material (3.04 g/cm^3 and 800 ± 70 HV). Fig. 12 shows a comparison between a green and a sintered part, where the shrinkage due to the binder removal is illustrated. In Table 6, sintering conditions, density, shrinkage and mechanical properties are summarized.

Table 6 – Sintering conditions, density and mechanical properties of the sintered P3 porcelain parts.

Sintering temperature (°C)	1410
Sintering time (h)	1
Sintering atmosphere	Air
Density (g cm^{-3})	3.04
Linear shrinkage (%)	15
Vickers hardness (HV)	800 ± 70
Bending strength (MPa)	200 ± 20

The results concerning hardness and bending strength are particularly remarkable especially when compared with conventional technical ceramics, such as alumina and zirconia, which are more expensive than the suggested porcelain material. In fact, a dramatic cost reduction in ceramic manufacturing of complex components can be expected by replacing the more expensive raw materials with the presented P3 porcelain which could be interesting for a variety of applications, aesthetic and electrical among others [32]. Finally, a microstructural characterization was carried out by SEM and results are displayed in Fig. 13. Microstructure is in accordance with the conventional features of porcelains. Different crystalline phases are identified embedded into a silica-rich glass phase (dark grey coloured) and porosity. Regarding the crystalline phases, the round shaped particles can be associated with quartz, while the trapezoidal particles are related to mullite and corundum crystallized phases. Porosity has a considerable influence on the technological features, mostly on the mechanical properties. In the case of the P3 microstructure the porosity found is very rare, closed and round shaped. During the sintering process, the development of liquid phase is progressively closing the capillaries that constituted the open porosity. The larger isolated pores with a spherical shape (>10 μm) found are directly linked to the melting of the feldspar grains. Coarse closed porosity is mostly

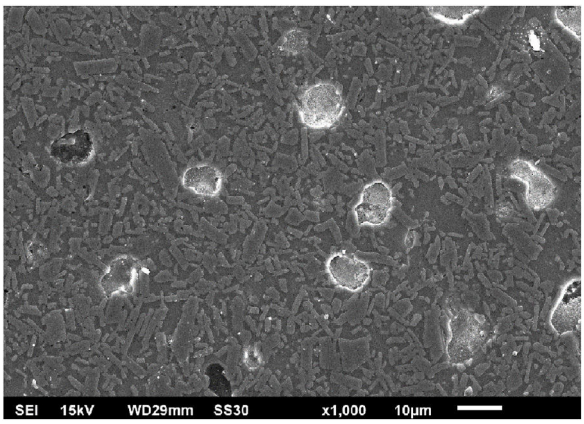

Fig. 13 – SEM micrograph of the P3 porcelain microstructure after sintering at 1410 °C and the different phases identified.

associated to the stain resistance because when the porcelain is polished, the closed porosity is exposed at the surface [33]. There is no evidence of interparticle porosity, which is the most critical in the mechanical strength, since it is considered stress concentrator, and which could facilitate fracture. Concerning the glass phase content on mechanical properties of porcelain, there are controversial results because the role during the sintering process is not fully understood yet, although there are evidences that the viscous phase is governing the densification kinetics during the sintering process. On the other side, the quartz particles seem to have a decisive contribution on the fracture energy and the mullite could be the responsible for the strength. Consequently, bending strength used to increase with increasing amount of mullite crystals. In conclusion, the observed microstructure, obtained by CIM process, is in good agreement with the mechanical properties measured and the mechanism of formation described in the peer reviewed literature for sintered porcelain system [33].

Conclusions

The viability of processing three different types of porcelain powders by CIM has been investigated. Porcelain P1, showing spherical shape, the lowest particle size and the narrowest particle size distribution, became difficult to mix with the studied binder at 45 vol.% ceramic content. Contrary to P1, porcelains P2 and P3 presented irregular shape and higher particle size. Despite this, P2 and P3 feedstocks resulted in being homogeneously mixed under the same mixing conditions and ceramic content. The optimal solids loading was defined for each case according to torque and MFI studies. However, reproducibility of the mixing behaviour after preparing similar feedstocks several times was higher in the case of porcelain P3. Moreover, a higher maximization of solids loadings was accomplished with P3, confirming that the more angular shaped, higher particle size and non-gaussian particle size distribution of P2 hindered an efficient powder packing and disfavoured the injection moulding step. Thus, the best results in terms of feedstock homogeneity and injection process reliability were obtained with the porcelain P3. Furthermore, the viscosity of P3 feedstocks was adapted for both low- and high-pressure injection PIM processes, resulting in a successful scale up of the designed composition, that it was even reformulated, to larger production at an industrial level. After debinding and sintering optimization, high quality porcelain components were obtained showing remarkable mechanical properties and adequate microstructure. These results demonstrate the viability of this novel low-cost porcelain feedstock for its use in some of the typical applications for alumina and zirconia ceramics with very complex geometry.

Acknowledgements

This work has been financed by a UCTR150442 contract with BSH Electrodomésticos España and supported by Vicar S. A. collaboration.

REFERENCES

[1] D.F. Heaney, Handbook of Metal Injection Molding, Woodhead Publishing, UK, 2012.
[2] B.C. Mutsuddy, R.G. Ford, Ceramic Injection Moulding, Chapman & Hall, UK, 1995.
[3] R.M. German, A. Bose, Injection Molding of Metals and Ceramics, Metal Powder Industries Federation, USA, 1997.
[4] N. Williams, PIM International, 12 (March 2018) 1–108.
[5] M.J. Edirisinghe, J.R.G. Evans, Review: Fabrication on engineering ceramics by injection moulding. II. Techniques, Int. J. High Technol. Ceram. 2 (1986) 249–278.
[6] I. Agote, A. Odriozola, M. Gutierrez, A. Santamaría, J. Quintanilla, P. Coupelle, J. Soares, Rheological study of waste porcelain feedstocks for injection moulding, J. Eur. Ceram. Soc. 21 (2001) 2843–2853.
[7] J.W. Wang, Wax-based polyethylene polymer binder is molded by injection of aluminium oxide porcelain composed of paraffin, low-density polyethylene and stearic acid having predetermined component and volume part ratio, CN101456742-A, 2007.
[8] I. Santacruz, M.I. Nieto, R. Moreno, P. Ferrandino, A. Salomoni, I. Stamenkovic, Aqueous injection moulding of porcelains, J. Eur. Ceram. Soc. 23 (2003) 2053–2060.
[9] K. Schindler, A. Roosen, T. Jüttner, G. Rösler, Wet-pressing of handles in table porcelain manufacturing, J. Eur. Ceram. Soc. 27 (2007) 1889–1892.
[10] D.F. Heaney, Powders for metal injection molding (MIM), in: D.F. Heaney (Ed.), Handbook of Metal Injection Molding, Woodhead Publishing, UK, 2012, pp. 50–63.
[11] J.K. Wright, M.J. Edirisinghe, J.G. Zhang, J.R.G. Evans, Particle packing in ceramic injection molding, J. Am. Ceram. Soc. 73 (1990) 2653–2658.
[12] W. Liu, J. Wen, Z. Xiw, X. Yang, Powder modification mechanism, effects of binder compositions on the thermal behavior, and the mechanical properties of the ceramic injection molded system, Ceram. Int. 44 (2018) 5646–5651.
[13] W.J. Tseng, D.-M. Liu, C.-K. Hsu, Influence of stearic acid on suspension structure and green microstructure of injection-molded zirconia ceramics, Ceram. Int. 25 (1999) 191–195.
[14] S.T. Paulin, R.M. German, The influence of powder loading and binder additive on the properties of alumina injection-moulding blends, J. Mater. Sci. 29 (1994) 5367–5373.

[15] K.M. Kulkarni, Dimensional precision of MIM parts under production conditions, Int. J. Powder Metall. 33 (1997) 29–41.
[16] R. Supati, N.H. Loh, K.A. Khor, S.B. Tor, Mixing and characterization of feedstock for powder injection molding, Mat. Lett. 46 (2000) 109–114.
[17] P. Thomas-Vielma, A. Cervera, B. Levenfeld, A. Várez, Production of alumina parts by powder injection molding with a binder system based on high density polyethylene, J. Eur. Ceram. Soc. 28 (2008) 763–771.
[18] A. Arifin, A.B. Sulong, Effect of mixing parameters on the mixing time and density of composite HA/Ti6Al4V feedstock for powder injection molding, MATEC Web Conf. 101 (2017) 1–5.
[19] H. Abdoos, H. Khorsand, A.A. Yousefi, Torque rheometry and rheological analysis of powder–polymer mixture for aluminum powder injection molding, Iran, Polym. J. 23 (2014) 745–755.
[20] A. Márquez, J. Quijano, M. Gaulin, A calibration technique to evaluate the power-law parameters of polymer melts using a torque-rheometer, Polym. Eng. Sci. 36 (1996) 2556–2563.
[21] M.J. Edirisinghe, J.R.G. Evans, Properties of ceramic injection moulding formulations, J. Mater. Sci. 22 (1987) 269–277.
[22] J. A. Mangels, W. Trela. Ceramic components by injection molding, Adv. in Ceram. 9 (1984) 220–233, Proceedings of a Special Conference of the 85th Annual Meeting of the American Ceramic Society, USA.
[23] N. Sa'ude, M. Ibrahim, M.H.I. Ibrahim, Melt flow rate (MFR) of ABS-copper composite filament by Fused Deposition Modeling (FDM), ARPN J. Eng. Appl. Sci. 11 (2016) 6562–6567.
[24] G. Thavanayagam, K.L. Pickering, J.E. Swan, P. Cao, Analysis of rheological behaviour of titanium feedstocks formulated with a water-soluble binder system for powder injection moulding, Powder Tech. 269 (2015) 227–232.
[25] C. Karatas, A. Kocer, H.I. Ünal, S. Saritas, Rheological properties of feedstocks prepared with steatite powder and polyethylene-based thermoplastic binders, J. Mater. Proc. Tech. 152 (2004) 77–83.
[26] A. Romero, G. Herranz, Development of feedstocks based on steel matrix composites for metal injection moulding, Powder Technol. 308 (2017) 472–478.
[27] K. García-Aguirre, J.L. Felguera-Jiménez, G. Herranz, J. Calvo-Muñoz, J.A. Benito-Páramo, J.M. Cabrera-Marrero, Metal injection moulding (MIM) as an alternative fabrication process for the production of TWIP steel, Powder Metall. 62 (3) (2019) 205–211.
[28] E. Enríquez, C. Berges, V. Fuertes, A. Gallego, J.A. Naranjo, G. Herranz, J.F. Fernández, Ceramic Injection Moulding of engineered glass-ceramics: boosting the rare-earth free photoluminescence, Ceram. Int. (2019) (in press).
[29] R.K. Enneti, V.P. Onbattuvelli, S.V. Atre, Powder binder formulation and compound manufacture in metal injection molding (MIM), in: D.F. Heaney (Ed.), Handbook of Metal Injection Molding, Woodhead Publishing, UK, 2012, pp. 64–92.
[30] A. Mannschatz, A. Müller, T. Moritz, Influence of powder morphology on properties of ceramic injection moulding feedstocks, J. Eur. Ceram. Soc. 31 (2011) 2551–2558.
[31] R. Zauner, D.F. Heaney, J.C. Piemme, C. Binet, R.M. German, The Effect of Powder Type and Powder Size on Dimensional Variability in PIM, Advances in Powder Metallurgy and Particulate Materials, Orlando, Publ. MPIF, Princeton, NJ, USA, Part 10, 2002, pp. 191–198.
[32] Y. Dong, S. Chen, X. Zhang, J. Yang, X.G. Liu, Meng., Fabrication and characterization of low cost tubular mineral-based ceramic membranes for micro- filtration from natural zeolite, J. Membr. Sci. 281 (2006) 592–599.
[33] M. Romero, J.M. Pérez, Relation between the microstructure and technological properties of porcelain stoneware. A review, Materiales de Construcción 65 (Issue 320.) (2015).